



## Energy and exergy analysis of single slope passive solar still: an experimental investigation

Sivakumar Vaithilingam<sup>a,\*</sup>, Ganapathy Sundaram Esakkimuthu<sup>b</sup>

<sup>a</sup>Department of Mechanical Engineering, R.M.K. Engineering College, Chennai 601206, India, email: [vsk.mech@rmkec.ac.in](mailto:vsk.mech@rmkec.ac.in)

<sup>b</sup>Department of Mechanical Engineering, Velammal Engineering College, Chennai 600066, India, email: [ganapathy\\_sundar@yahoo.com](mailto:ganapathy_sundar@yahoo.com)

Received 11 October 2013; Accepted 16 May 2014

### ABSTRACT

Exergy analysis is a powerful indicative tool for thermal systems performance evaluation. Now a day, there has been an increasing interest in using exergy as a prospective tool for analysis. In this paper, an attempt is made to perform energy and exergy analysis of single slope passive solar still of size of  $1 \times 0.5$  m with the glass thickness 5 mm and slope  $13^\circ$ . To examine the effects of water depth for same total daily solar intensity on energy and exergy efficiency, experiments were carried out at Chennai ( $13^\circ 5' 2''$  N,  $80^\circ 16' 12''$  E), Tamil Nadu, India. The exergy destruction of different components of solar still for various water depths was also determined. The study found that the highest exergy destruction is takes place in basin liner as compared with the other components for all the water depths.

*Keywords:* Passive solar still; Water depth; Energy efficiency; Exergy efficiency; Exergy destruction

### 1. Introduction

Drinking water is a basic necessity for human beings along with food and air. The presence of high amount of salt and contamination in water from sources like sea, lakes, rivers, and underground water reservoir makes it unsuitable for use directly. The demand for fresh water is growing steadily and has become a worldwide challenge. Desalination is the process of bringing down the salinity of seawater or brackish water from a high level of total dissolved solids of 35,000 ppm to an acceptable level of 500 ppm [1]. One of the gifted options for eliminating the major operating cost of desalination plant is direct use of solar energy. Solar still is a simple device which converts available water or brackish water into potable

water using solar energy. The easily available solar energy is clean, plentiful, and renewable. Solar stills can be used for low capacity and self-reliance water supply systems [2]. Solar stills are cheap and have low-maintenance cost but have the problem of low productivity. The methodologies used to improve the performance of the active and passive solar stills were reviewed by many researchers [3].

Torchia-Nunez et al. [4] theoretically analyzed the exergy destruction in the components of a passive solar still: collector plate, brine, and glass cover under steady-state conditions. The study found that the exergy efficiency of 12.9, 6, and 5% for the collector, brine, and solar still, respectively, for the same exergy input and mentioned that the collector plate produces the greater irreversibility rate as compared with brine and glass cover. Tiwari et al. [5] studied the effect of inner ( $T_{gi}$ ) and outer ( $T_{go}$ ) glass cover temperatures on the

\*Corresponding author.

performance of the active and passive solar still based on the computer thermal modeling. The extended study also covers the effect of the water depth and the number of collectors on energy and exergy efficiency of the active solar still. The exergy efficiency of 1.71% was obtained at 5 cm water depth when desalination system incorporated with three solar collectors. The study reveals that energy efficiency decreases with increase in water depth and number of collectors however, the exergy efficiency has an insignificant change. For a single collector, the energy and exergy efficiency decreases from 11.21 to 5.62% and 1.6 to 0.5%, respectively, when the water depth increases from 5 to 15 cm.

Dwivedi and Tiwari [6] presented the hourly thermal and exergy efficiency of active solar still containing 0.03 m water depth for the climate of Ghaziabad (Latitude 28°40'N, Longitude 77°25'E). The double slope active solar still under natural modes gives 51% higher yield in comparison with the double slope passive solar still. The thermal efficiency of double slope active solar still is lower than the thermal efficiency of double slope passive solar still. However, the exergy efficiency of double slope active solar still is higher than the exergy efficiency of double slope passive solar still. The daily yield of a double slope passive solar still for a particular day in the month of March 2008 was found to be 1.838 kg/m<sup>2</sup>, whereas the daily yield of a double slope active solar still under natural mode was found to be 2.791 kg/m<sup>2</sup>. The overall average thermal and exergy efficiencies of flat plate collector integrated active solar still were 10.34 and 1.16%, respectively.

An analytical expression for instantaneous exergy efficiency of a shallow basin passive solar still was developed by Kumar and Tiwari [7]. It was found that the energy and exergy efficiencies were decreased by 21.8% and 36.7%, respectively, when the absorptivity of basin liner decreases from 0.9 to 0.6. The exergy efficiency increased rapidly with wind velocity up to 2 m/s and further increase of wind velocity decreased exergy efficiency. Shanmugan et al. [8] experimentally studied the performance of single slope basin type solar still at Coimbatore (Latitude 11°N, Longitude 77°52'E) and evaluated the instantaneous energy and exergy efficiency of the still. The instantaneous energy efficiency is greater than the instantaneous exergy efficiency. The instantaneous energy efficiency varies from 32 to 57% in summer and 12 to 60% in winter. The instantaneous exergy efficiency varies from 7 to 18% in summer and 6 to 19% in winter.

Kianifar et al. [9] conducted experiments in Mashhad (36°36'N) using two units of a pyramid-shaped active (equipped with small fan) and passive (no fan) solar still

for revealing exergy and economic analysis. In the passive solar still for 4 cm water depth, the daily exergy efficiency found to be 3.06% in summer and 2.43% in winter. For the summer, when the water depth increases from 4 to 8 cm, the daily exergy efficiency decreased from 3.06% to 2.81%. Sethi and Dwivedi [10] conducted experiments at Greater Noida on double slope active solar still under forced circulation mode. It was observed that the daily thermal efficiency of solar still varies from 13.55 to 31.07% and the exergy efficiency varies from 0.26 to 1.34%.

Ranjan et al. [11] carried out energy and exergy analysis of a passive solar still for climatic conditions of Udaipur. The daily energy, exergy, global exergy efficiency, and distillate yield are found to be 30.42%, 4.93%, 23.14%, and 4.17 l/d, respectively, for 1 cm water depth with total solar radiation of 7,446 W/m<sup>2</sup> from 7.00 am to 6.00 pm. Moreover, the exergy destruction of solar still components such as basin liner, saline water, and glass cover is evaluated as 3,353, 1,633, and 362 W/m<sup>2</sup>/d, respectively.

Ranjan and Kaushik [12] reviewed energy, exergy, and thermodynamic analysis of solar distillation systems. It is observed that the energy efficiency of the conventional solar still is in the range of 20–46% and productivity is less than 6 l/m<sup>2</sup>/d. Also, the exergy efficiency of a single effect system is less than 5% and this value will reach up to 8.5% for the integrated solar still. In economic point of view, the cost of desalination decreases with increase in solar still efficiency. The cost of desalination per liter through solar still is estimated in the range of US\$0.014–0.237.

Aghaei Zoori et al. [13] studied theoretically and experimentally the energy and exergy efficiencies of cascade solar still and found that 84.17% of the total irreversibility (310.01 W) is shared by the absorber plate (260.97 W). The second highest contribution from glass cover is 43.45 W and the least contribution from saline water is 5.62 W. The energy and exergy efficiency of the system increases from 44.1 to 83.3% and 3.14 to 10.5%, respectively, when the inlet brine flow rate decreases from 0.2 to 0.065 kg/min.

Ansari et al. [14] highlighted the effect of heat energy storage on the desalination of the brackish water using a passive solar still with three kinds of paraffin. The melting temperature of paraffins is 42, 52, and 56 °C. The heat storage with 56 and 52 °C melting temperature paraffins gives 40% higher water yield and 42 °C gives 8% higher water yield.

An experimental and theoretical energy and exergy analysis for a solar desalination system consisting of a solar collector and a humidification tower was carried out by Nematollahi et al. [15]. The results point out that overall exergy efficiency of the system decreases

with an increase in the humidification tower length and increases with a decrease in inlet air temperature and tower diameter. A comprehensive literature review on exergy analysis of various solar energy applications such as solar photovoltaic, solar pond, solar heating devices, solar water desalination, solar air conditioning and refrigeration, solar drying process, and solar power generation was carried out by Saidur et al. [16]. BoroumandJazi et al. [17] reviewed the relation between the energy and exergy efficiency analysis and the technical characteristic of the renewable energy system. The review concluded that the systems which are more reliable and sustainable have less environmental impact and high energy and exergy efficiencies. A relationship between entropy generation maximum principle and the exergy analysis of engineering and natural systems was made by Lucia [18] which is used to improve the renewable energy systems.

The methodology and results reported by the above mentioned researchers motivated us to study the energy and exergy analysis of single slope passive solar still and identify the exergy destruction of its various components under Chennai climatic conditions. In this view, a single slope passive solar still has been fabricated. The experiments were conducted for different days (different solar intensity) with different water depths. For the water depths of 1, 1.5, 2, and 2.5 cm with same total daily solar intensity data have been taken for performance analysis for finding the effects of water depth on energy and exergy efficiencies and exergy destruction of various components of the solar still.

## 2. Experimental setup

The pictorial view of single slope passive solar still is shown in Fig. 1a. The specifications of the still are given in the Table 1. Single slope passive solar still of basin area  $1 \times 0.5$  m was fabricated using stainless steel Grade 304. The basin surface is painted black to absorb the maximum amount of solar radiation incident on them. The condenser surface of the still is made of glass 5-mm thickness and angle of inclination is  $13^\circ$  with horizontal (latitude of Chennai). The dimensions of the solar still are shown in Fig. 1b. Solar still was placed in east–west direction to receive maximum possible solar radiation. The entire basin still is kept inside the wooden frame and good insulating material such as 25.4-mm thick thermocol is placed between the still and wooden frame. A collecting trough made by stainless steel is used in the still to collect the distillate condensing on the inner surfaces of the glass covers and to pass the condensate to



Fig. 1a. Pictorial view of the experimental setup.

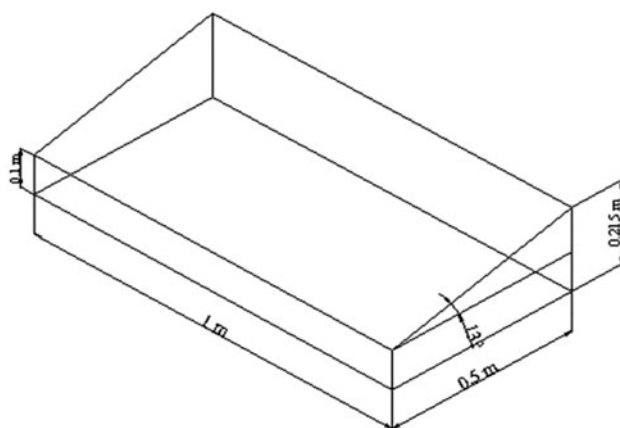


Fig. 1b. Dimensions of the single slope passive solar still.

Table 1  
Specifications of single slope passive solar still

S. No.	Dimensions	Measurements
1	Length	1 m
2	Width	0.5 m
3	Glass cover inclination	$13^\circ$
4	Depth of basin at front side	0.215 m
5	Depth of basin at back side	0.100 m
6	Thickness of glass cover	5 mm

a collecting flask with least count of 1 ml. Calibrated thermocouples with the range of  $0\text{--}700^\circ\text{C}$  and an accuracy of  $\pm 1^\circ\text{C}$ , connected to a multi-channel digital temperature indicator are inserted through the holes provided in the sides of the still and fixed at different points to measure the temperatures of different parts of the still like basin, water, inner and outer surfaces

of the glass, and ambient temperature. To keep the whole system vapor tight, putty is used as sealant because it would remain elastic for quite long time. The intensity of solar radiation is measured using solarimeter, having least count of  $1 \text{ W/m}^2$  with the range of  $0\text{--}2,000 \text{ W/m}^2$  and accuracy  $\pm 5 \text{ W/m}^2$ .

### 3. Experimental observations

The experiments were conducted at Velammal Engineering College, Chennai ( $13^\circ 5' 2'' \text{N}$ ,  $80^\circ 16' 12'' \text{E}$ ), Tamil Nadu, India, from February 2013 to April 2013 during 9 am to 5 pm (daylight hours). The solar intensity on solar still, ambient temperature, saline water temperature, basin temperature, inner and outer glass temperature, and distilled water output are measured at regular intervals of 1 h. Performance of single slope passive solar still is investigated at water depth of 1, 1.5, 2, and 2.5 cm. The saline water is poured inside the still one hour before the start of the experiment and the readings were taken from 9 am to 5 pm with one hour time interval. From the experimental data, the water depth of 1, 1.5, 2, and 2.5 cm with same total daily solar intensity ( $\sim 6,250 \text{ W/m}^2$ ) has been taken for analysis. Design parameters used for energy and exergy analysis, in this paper, are presented in

Table 2 and the average experimental observations for different water depths are given in Table 3.

#### 3.1. Thermal analysis of passive solar still

According to energy analysis, energy utilization processes have been evaluated based on the first law of thermodynamics. The solar still daily efficiency,  $\eta_{\text{energy}}$ , is obtained by summing up the hourly condensate production multiplied by the latent heat of vaporization, and divided by the daily total solar intensity over the solar still area and calculated from the following Eqs. ((1) and (2)) [19]:

The daily yield ( $M_w$ ) can be obtained by adding hourly yield from 9 am to 5 pm.

$$M_w = \left( \sum_{i=1}^{i=9} m_w \right) \quad (1)$$

$m_w$  = hourly distillate yield in kg.

$$\eta_{\text{energy}} = \frac{M_w \times L}{\left( A_s \times \sum_{t(s)} I_{t(s)} \times 3,600 \right)} \quad (2)$$

where  $L$  is given by Eq. (3) [20].

Table 2  
Design parameters used for energy and exergy analysis

S. No.	Parameter	Value
1	Absorptivity of glass cover ( $\alpha_g$ ) [13]	0.05
2	Absorptivity of basin liner ( $\alpha_b$ ) [13]	0.9
3	Absorptivity of water ( $\alpha_w$ ) [13]	0.05
4	Transmissivity of glass cover ( $\tau_g$ ) [13]	0.9
5	Transmissivity of water ( $\tau_w$ ) [13]	0.95
6	Effective emissivity ( $\epsilon_{\text{eff}}$ ) [26]	0.82
7	Thermal conductivity of Insulating material ( $K_{\text{ins}}$ )	$0.015 \text{ W/m K}$
8	Heat transfer coefficient between basin liner and water surface ( $h_w$ ) [22]	$135 \text{ W/m}^2 \text{ K}$
9	Overall heat transfer coefficient between basin liner and atmosphere ( $h_b$ ) [22]	$14 \text{ W/m}^2 \text{ K}$
10	Stefan—Boltzmann constant $\sigma$	$5.67 \times 10^{-8} \text{ W/m}^2 \text{ K}^4$

Table 3  
Average ambient temperature, water temperature, solar intensity, daily yield, energy efficiency, exergy evaporated and exergy efficiency for single slope passive solar still for different water depth

Date of experiment (in the year 2013)	Water depth (cm)	Temperature ( $^\circ \text{C}$ )		$\sum I_{t(s)}$ ( $\text{W/m}^2$ )	$M_w$ (kg)	Energy efficiency (%)	Exergy evaporated (W)	Exergy efficiency (%)
		$T_a$	$T_w$					
13 March	1	32.4	62.3	6,255	1.485	30.96	101.15	3.48
22 March	1.5	34.1	61.1	6,261	1.333	27.80	79.07	2.72
4 April	2	35	61.7	6,237	1.247	26.10	72.82	2.51
18 April	2.5	35.9	61.9	6,249	0.920	19.21	52.46	1.81

$$L = 2.4935 \times 10^6 \times [1 - 9.4779 \times 10^{-4} T_w + 1.3132 \times 10^{-7} \times T_w^2 - 4.794 \times 10^{-9} \times T_w^3] \quad (3)$$

$T_w$  is basin water temperature in °C.

### 3.2. Exergy analysis of passive solar still

Exergy analysis is derived from the second law of thermodynamics. Exergy of a thermodynamic system is the part of energy which is the maximum useful work that can be obtained from the system at a given state in a specified environment. Exergy efficiency is calculated from the following Eqs. ((4)–(10)) [10]:

$$\sum \dot{E}_{x_{in}} - \sum \dot{E}_{x_{out}} = \sum \dot{E}_{x_{dest}} \quad (4)$$

$$\sum \dot{E}_{x_{sun}} - (\sum \dot{E}_{x_{evap}} + \sum \dot{E}_{x_{work}}) = \sum \dot{E}_{x_{dest}} \quad (5)$$

$$\begin{aligned} \sum \dot{E}_{x_{in}} &= \sum \dot{E}_{x_{sun}} \\ &= \left( A_s \times \sum I_{t(s)} \right) \\ &\quad \times \left[ 1 - \frac{4}{3} \times \left( \frac{T_a + 273}{T_s} \right) + \frac{1}{3} \times \left( \frac{T_a + 273}{T_s} \right)^4 \right] \end{aligned} \quad (6)$$

$$\sum \dot{E}_{x_{work}} = \dot{W} = 0 \quad (7)$$

$$\sum \dot{E}_{x_{evap}} = \frac{M_w \times L \times \left[ 1 - \left( \frac{T_a + 273}{T_w + 273} \right) \right]}{3,600} \quad (8)$$

The exergy efficiency can be calculated as the ratio between the net exergy output and the input exergy.

$$\eta_{Ex} = \frac{\sum \dot{E}_{x_{evap}}}{\sum \dot{E}_{x_{sun}}} \quad (9)$$

$$\eta_{Ex} = 1 - \frac{\dot{E}_{x_{dest}}}{\dot{E}_{x_{sun}}} \quad (10)$$

### 3.3. Exergy destruction of solar still components

The combination of conservation of law of energy and non-conservation of exergy is used for finding exergy balance for any system or its components [21]. The exergy balance Eqs. ((11), (15), and (24)) of the three main components of the solar still such as

basin—liner, saline water, and glass cover are given below [11].

#### 3.3.1. Basin liner

The exergy input for the basin liner is the fraction of solar exergy ( $E_{x_{sun}}$ ) reaching on it. The useful exergy is utilized to raise the temperature of saline water ( $E_{x_w}$ ) and a little is lost through insulation ( $E_{x_{ins.}}$ ) and remaining is destroyed ( $E_{x_{des.,b}}$ ).

$$E_{x_{des.,b}} = (\tau_g \tau_w \alpha_b) E_{x_{sun}} - (E_{x_w} + E_{x_{ins.}}) \quad (11)$$

$\tau_g$ ,  $\tau_w$  and  $\alpha_b$  transmittance of the glass cover, saline water, and absorptivity of the basin—liner [13], respectively.

Exergy of the solar radiation on the solar still per unit area,  $E_{x_{sun}}$  (W/m<sup>2</sup>), is given as:

$$E_{x_{sun}} = I_{t(s)} \left[ 1 + \frac{1}{3} \left( \frac{T_a}{T_s} \right)^4 - \frac{4}{3} \left( \frac{T_a}{T_s} \right) \right] \quad (12)$$

$T_a$  is the temperature of the atmosphere outside the solar still (K) and  $T_s$  is the temperature of the sun (5,777 K).

$$E_{x_w} = h_w (T_b - T_w) \left( 1 - \frac{T_a}{T_b} \right) \quad (13)$$

where  $h_w$  [22] is the convective heat transfer coefficient between basin liner and saline water (W/m<sup>2</sup> K).  $T_b$  is the temperature of the basin (K) and  $T_w$  is the temperature of the saline water (K).

$$E_{x_{ins.}} = h_b (T_b - T_a) \left( 1 - \frac{T_a}{T_b} \right) \quad (14)$$

where  $h_b$  [22] is the overall heat transfer coefficient between basin liner and atmosphere (W/m<sup>2</sup> K).

#### 3.3.2. Saline water

The exergy input for the saline water is the sum of the fraction of solar exergy ( $\tau_g \alpha_w E_{x_{sun}}$ ) absorbed by water and the useful exergy from the basin liner which is utilized to raise the temperature of saline water ( $E_{x_w}$ ). A part of it is utilized as the exergy associated with the heat transfer between saline water surface and the inner side of the glass cover  $E_{x_{l,w-g}}$  and remaining is destroyed ( $E_{x_{des.,w}}$ ).

$$E_{x_{des,w}} = (\tau_g \alpha_w) E_{x_{sun}} + E_{x_w} - E_{x_{t,w-g}} \quad (15)$$

where  $\alpha_w$  [13] is the absorptivity of saline water and  $E_{x_{t,w-g}}$  is calculated as follows.

$$E_{x_{t,w-g}} = E_{x_{e,w-g}} + E_{x_{c,w-g}} + E_{x_{r,w-g}} \quad (16)$$

$E_{x_{e,w-g}}$ ,  $E_{x_{c,w-g}}$  and  $E_{x_{r,w-g}}$  are the exergy associated with the heat transfer through evaporation, convection, and radiation between the saline water surface and the inner side of the glass cover.

$$E_{x_{e,w-g}} = h_{e,w-g} (T_w - T_{gi}) \left( 1 - \frac{T_a}{T_w} \right) \quad (17)$$

where  $h_{e,w-g}$  is the evaporative heat transfer coefficient between saline water and inner side of the glass cover ( $\text{W}/\text{m}^2 \text{K}$ ) [23] and  $T_{gi}$  is the glass inner surface temperature (K).

$$h_{e,w-g} = 0.016273 h_{c,w-g} \frac{P_w - P_{gi}}{T_w - T_{gi}} \quad (18)$$

where  $P_w$  and  $P_{gi}$  are the partial pressures in ( $\text{N}/\text{m}^2$ ) for water vapor at water and the inner glass surface temperatures within the still which are given by [24] as:

$$P(T) = \exp \left[ 25.317 - \frac{5,144}{T} \right] \quad (19)$$

$$E_{x_{c,w-g}} = h_{c,w-g} (T_w - T_{gi}) \left( 1 - \frac{T_a}{T_w} \right) \quad (20)$$

where  $h_{c,w-g}$  is the convective heat transfer coefficient between saline water and inner side of the glass cover ( $\text{W}/\text{m}^2 \text{K}$ ) [23].

$$h_{c,w-g} = 0.884 \left[ T_w - T_{gi} + \frac{(P_w - P_{gi}) T_w}{268,900 - P_w} \right]^{1/3} \quad (21)$$

$$E_{x_{r,w-g}} = h_{r,w-g} (T_w - T_{gi}) \left[ 1 + \frac{1}{3} \left( \frac{T_a}{T_w} \right)^4 - \frac{4}{3} \left( \frac{T_a}{T_w} \right) \right] \quad (22)$$

where  $h_{r,w-g}$  is the radiative heat transfer coefficient between saline water and inner side of the glass cover ( $\text{W}/\text{m}^2 \text{K}$ ) [25].

$$h_{r,w-g} = \epsilon_{\text{eff}} \sigma (T_w^2 + T_{gi}^2) (T_w + T_{gi}) \quad (23)$$

$\epsilon_{\text{eff}}$  is the effective emissivity [26] and  $\sigma$  is the Stefan-Boltzmann constant taken as  $5.67 \times 10^{-8} \text{W}/\text{m}^2 \text{K}^4$ .

### 3.3.3. Glass cover

The exergy input for the glass cover is the sum of the fraction of solar exergy ( $\alpha_b E_{x_{sun}}$ ) absorbed by glass cover and the exergy associated with the heat transfer between saline water surface and the inner side of the glass cover ( $E_{x_{t,w-g}}$ ). A part of this exergy is lost in the atmosphere by convection and radiation heat transfer and remaining is destroyed ( $E_{x_{des,g}}$ ).

$$E_{x_{des,g}} = \alpha_g E_{x_{sun}} + E_{x_{t,w-g}} - E_{x_{t,g-a}} \quad (24)$$

where  $\alpha_g$  [13] is the absorptivity of glass cover and  $E_{x_{t,g-a}}$  is calculated as follows:

$$E_{x_{t,g-a}} = E_{x_{c,g-a}} + E_{x_{r,g-a}} \quad (25)$$

$$E_{x_{c,g-a}} = h_{c,g-a} (T_{go} - T_a) \left( 1 - \frac{T_a}{T_{go}} \right) \quad (26)$$

$$h_{c,g-a} = 5.7 + 3.8 V \quad (27)$$

$V$  = wind speed in m/s.

where  $h_{c,g-a}$  is the convective heat transfer coefficient between glass cover and atmosphere ( $\text{W}/\text{m}^2 \text{K}$ ) [27] and  $T_{go}$  is the outer glass temperature (K).

$$E_{x_{r,g-a}} = h_{r,g-a} (T_{go} - T_a) \left[ 1 + \frac{1}{3} \left( \frac{T_a}{T_{go}} \right)^4 - \frac{4}{3} \left( \frac{T_a}{T_{go}} \right) \right] \quad (28)$$

where  $h_{r,g-a}$  is the radiative heat transfer coefficient between glass cover and atmosphere ( $\text{W}/\text{m}^2 \text{K}$ ) [27].

$$h_{r,g-a} = \frac{\epsilon_{\text{eff}} \sigma (T_{go}^4 - T_{\text{sky}}^4)}{T_{go} - T_{\text{sky}}} \quad (29)$$

$$T_{\text{sky}} = 0.0552 T_a^{1/5} \quad (30)$$

$T_{\text{sky}}$  is the sky temperature (K) [28].

### 3.4. Experimental uncertainty analysis

Uncertainty associated with the experimental measurements is shown in Table 4. The error is calculated for thermocouples, solarimeter, and measuring jar. The minimum error occurred in any instrument is equal to the ratio between its least count and minimum value of the output measured [9].

### 3.5. Mathematical uncertainty analysis

The result  $R$  is a given function of the independent variables  $x_1, x_2, x_3, \dots, x_n$ .

Thus,  $R = R(x_1, x_2, x_3, \dots, x_n)$ .

Let  $\omega_R$  be the uncertainty in the result and  $\omega_1, \omega_2, \omega_3, \dots, \omega_n$  be the uncertainties in the independent variables. If the uncertainties in the independent variables are all given with the same odds, then the uncertainty in the result having these odds is given as [29]:

$$\omega_R = \left[ \left( \frac{\partial R}{\partial x_1} \times \partial x_1 \right)^2 + \left( \frac{\partial R}{\partial x_2} \times \partial x_2 \right)^2 + \dots + \left( \frac{\partial R}{\partial x_n} \times \partial x_n \right)^2 \right]^{\frac{1}{2}} \tag{31}$$

If this relation is applied to the energy and exergy efficiency of the previous section,

$$\omega_{\eta_{\text{energy}}} = \left[ \left( \frac{\partial \eta_{\text{energy}}}{\partial m_w} \times \partial m_w \right)^2 + \left( \frac{\partial \eta_{\text{energy}}}{\partial T_w} \times \partial T_w \right)^2 + \left( \frac{\partial \eta_{\text{energy}}}{\partial \sum I_{(t)s}} \times \partial \sum I_{(t)s} \right)^2 \right]^{\frac{1}{2}} \tag{32}$$

$$\omega_{\eta_{\text{exergy}}} = \left[ \left( \frac{\partial \eta_{\text{exergy}}}{\partial m_w} \times \partial m_w \right)^2 + \left( \frac{\partial \eta_{\text{exergy}}}{\partial T_a} \times \partial T_a \right)^2 + \left( \frac{\partial \eta_{\text{exergy}}}{\partial T_w} \times \partial T_w \right)^2 + \left( \frac{\partial \eta_{\text{exergy}}}{\partial \sum I_{(t)s}} \times \partial \sum I_{(t)s} \right)^2 \right]^{\frac{1}{2}} \tag{33}$$

Table 4  
Experimental uncertainty errors

Instrument	Accuracy	Range	% Error
Thermocouples	±1 °C	0–700 °C	3.33
Solarimeter	±5 W/m <sup>2</sup>	0–2,000 W/m <sup>2</sup>	0.909
Measuring jar	±1 ml	0–250 ml	4.17

## 4. Results and discussion

The energy and exergy analysis of single slope passive solar still has been carried out with different water depths in this study. The energy and exergy efficiencies depend upon one of the meteorological parameter such as available solar radiation in the local climatic conditions. Solar radiation varies with respect to the day of experiment. The experiment date, total daily solar intensity, and water depths are shown in Fig. 2. During the experimental period, the total daily solar intensity was varied from 5,065 to 6,713 W/m<sup>2</sup>/d. The different water depths with same total daily solar intensity (~6,250 W/m<sup>2</sup>/d) is taken into account for the study of effect of water depths on energy, exergy efficiency, and irreversibility associated with different components of solar still. The experiments carried out on 13 March (1 cm), 22 March (1.5 cm), 4 April (2 cm), and 18 April (2.5 cm) have been taken for this study. In the other experimental days, total daily solar intensity is either higher or lower than the value of 6,250 W/m<sup>2</sup>/d.

Fig. 3 shows the variation of the solar intensity incident on solar still with local time for different water depths. The incident solar intensity is increasing up to 12 Noon from morning and thereafter it starts to decrease up to evening. The maximum solar intensity received by the solar still is 1,120 W/m<sup>2</sup> on 18 April 2013 (2.5 cm water depth) at 12 Noon.

Daily water productivity is illustrated in Fig. 4. During one hour time interval, the maximum mass of water vapor evaporation takes place between 12 Noon and 1 pm for all the water depths. The maximum one hour distillate output of 300 ml was obtained from 1 cm water depth. Solar still productivity is higher at lower water depth. This is caused by the faster

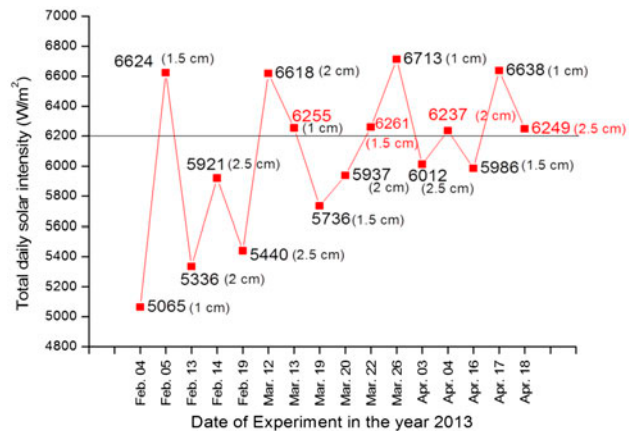


Fig. 2. Variation of total daily solar intensity in different days of experiments with water depths.

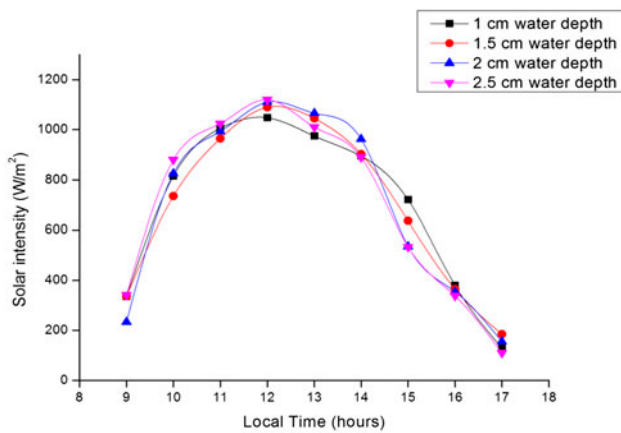


Fig. 3. Variation of solar intensity with local standard time for different water depths.

evaporation at lower water depth due to higher temperature difference between water and inner glass. It is also evident that when the water depth increases, the productivity decreased. This is due to the increase of heat capacity of the water in the basin, results in lower water temperature in the basin which leads to lower evaporation rate.

The evaporative heat flux is required to evaporate water from the water surface in the basin area. The exergy evaporation of the passive solar still is obtained by Eq. (8). Fig. 5 reveals that the exergy evaporated is more at 1 pm for all the water depths. These values are found to be 23.49, 20.40, 17.59, and 14.52 W for the water depth of 1, 1.5, 2, and 2.5 cm, respectively. At the lower water depth, the water thickness on the basin is small which results in increase in water temperature. As a result, evaporation is faster and the exergy evaporation is higher at lower water depth.

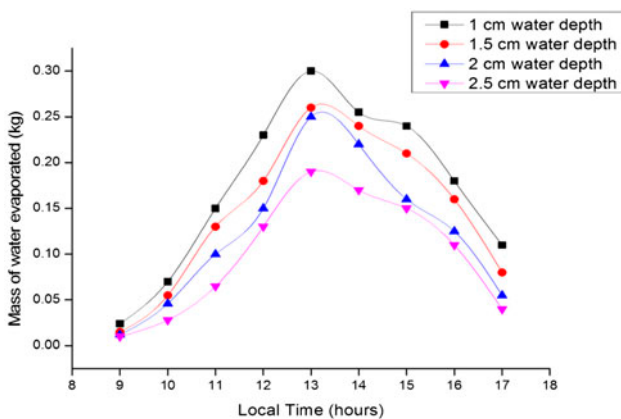


Fig. 4. The effect of water depth in the basin on the evaporation of water vapour.

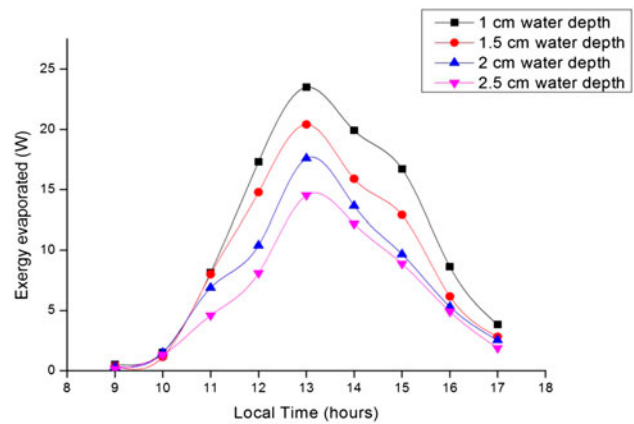


Fig. 5. Hourly variation of exergy evaporated for different water depths.

Hourly variation of exergy efficiency with different water depths has been presented in Fig. 6. The hourly exergy efficiency increases from the starting of the experiment up to 1 pm for all the water depths. Even though the incident solar intensity decreases from 1 pm the hourly exergy efficiency increases. This could be due to heat stored inside the water during higher incident solar intensity period (9 am to 1 pm). The maximum hourly exergy efficiency of 5.29% is achieved with 1-cm water depth at 3 pm. Due to more amount of heat stored in higher water depth the hourly exergy variation between 1.5, 2, and 2.5 cm water depth during 1 to 5 pm. is low as compared with lower water depth (1 cm).

The effect of water depth on energy efficiency and exergy efficiency for the same total daily solar intensity per day is shown in Fig. 7. The daily energy and

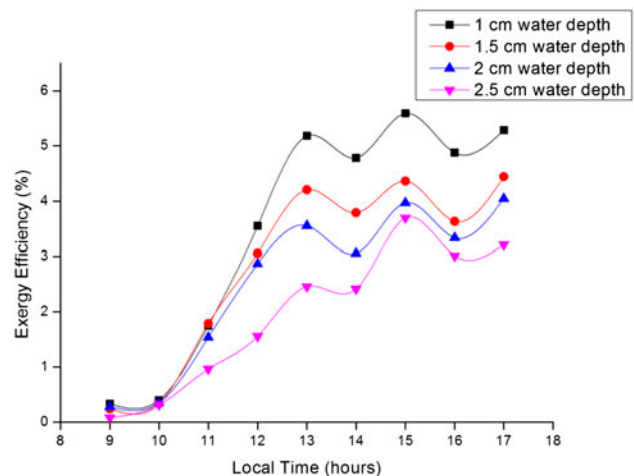


Fig. 6. Hourly variation of exergy efficiency for different water depths.

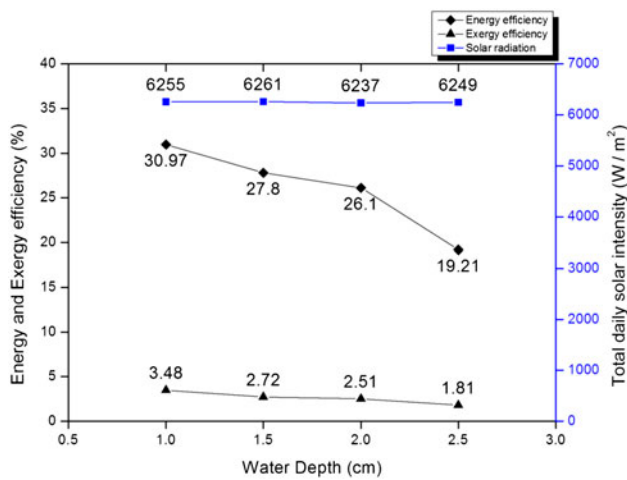


Fig. 7. Comparison of energy and exergy efficiency at different water depths for same total daily solar intensity.

exergy efficiency decreases from 30.97 to 19.2% and from 3.48 to 1.81%, respectively, when water depth increases from 1 cm to 2.5 cm. The exergy efficiency is lower than the energy efficiency for all the water depths. This is caused by the significant degradation of energy quality. The relatively high temperature (5,777 K) of solar radiation is degraded to the relatively low temperature e.g. to the temperature of heated water [12]. Similar trends (energy efficiency 30.58% and exergy efficiency 1.08%) are found in the experimental results available in literature [30]. The mathematical uncertainty value of energy and exergy efficiency is calculated from Eqs. (32) and (33) and the values are 0.145 and 3.79%, respectively.

The objective of exergy analysis is to find the quantity and location where exergy destruction takes place. This helps to improve the exergy efficiency by applying suitable measures and decrease the exergy destruction. In this study, the rate of instantaneous exergy destruction has been calculated for the components of passive solar still: basin liner, saline water, and glass cover. The Fig. 8 shows that the hourly variation of exergy destruction of various components. The maximum hourly rate of exergy destruction in basin liner, saline water, and glass cover are 544.12, 195.89, and 46.62 W/m<sup>2</sup>, respectively, for 1-cm water depth. Similar order of decreasing exergy destruction is found in literature [11]. It is observed that the largest exergy destruction takes place in the basin liner. This may be due to less temperature difference between basin liner and water ( $T_b - T_w$ ). The high-temperature difference between basin liner and water increases the exergy associated with water ( $E_{x_w}$ ) and decreases the exergy destruction in the basin liner. The second

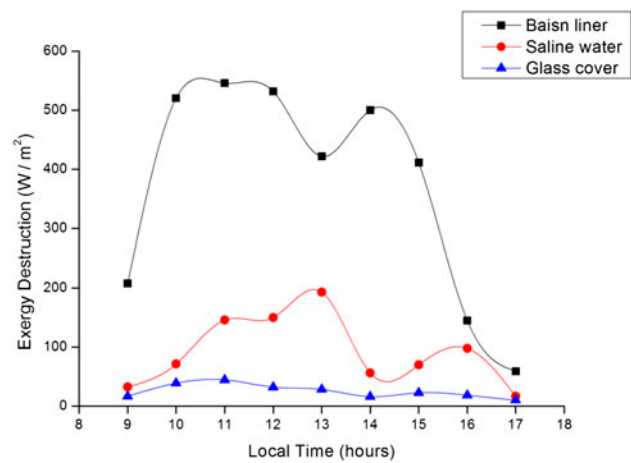


Fig. 8. Hourly variation of exergy destruction of solar still components at 1 cm water depth.

highest exergy destruction is attained in the saline water. The minimum exergy destruction of saline water can be obtained when the temperature difference between the water surface and inner glass temperature ( $T_w - T_{gi}$ ) is high. The higher temperature difference enhances the exergy evaporated ( $E_{x_{t,w-g}}$ ) from the water surface and reduces the exergy destruction of saline water. The temperature difference between the glass and atmosphere is less compared with other two components (basin liner and saline water) temperature difference with atmosphere. This leads to lower exergy destruction in the glass cover as compared with the basin liner and water.

The effect of water depth on exergy destruction of various solar still components is shown in Fig. 9. The rate of exergy destruction in the components is very much dependent on the rate of incident solar radiation. In the present work, the total daily solar intensity is almost constant ( $\sim 6,250$  W/m<sup>2</sup>) for all water depth. Therefore, the exergy of the solar radiation on the solar still per area ( $E_{x_{sun}}$ ) is also same. The exergy destruction from the basin liner increases from 3,343.89 to 3,933.68 W/m<sup>2</sup>/d when the water depth increases from 1 to 2.5 cm. The major cause of increase in exergy destruction with increase in water depth in the basin liner is due to lower rate of useful heat transfer from basin liner to saline water ( $E_{x_w}$ ). The exergy destruction of saline water decreases from 826.36 to 383.67 W/m<sup>2</sup>/d when the water depth increases from 1 to 2.5 cm. The major origin of decrease in exergy destruction with increase in water depth in the saline water is due to lower rise of water temperature in the basin when solar still is subjected to more water depth (quantity of water).

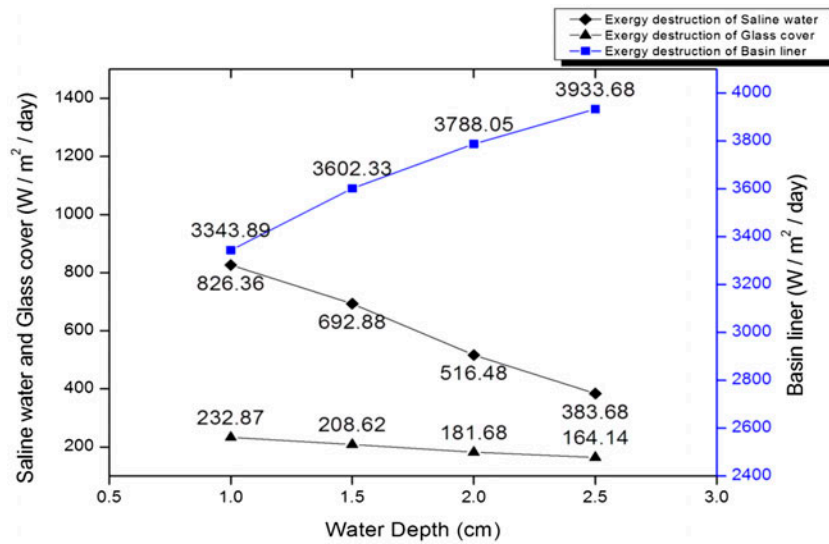


Fig. 9. Comparison of daily exergy destruction of solar still components at different water depths.

The exergy destruction of glass cover values is 232.87, 208.62, 181.68, and 164.14 W/m<sup>2</sup>/d for water depth of 1, 1.5, 2, and 2.5 cm, respectively. It reveals that the exergy destruction in the glass cover decreases with increase in water depth. The major cause of decrease in exergy destruction with increase in water depth in the glass cover is due to lower rate of total exergy associate with saline water and glass cover ( $E_{xt,w-g}$ ).

## 5. Conclusions

In this study, a single slope passive solar still is fabricated and analyzed to find the effect of water depths on energy efficiency and exergy efficiency for the same total daily solar intensity. Furthermore, the exergy destruction of different components of the solar still is also analyzed. The following conclusions can be drawn:

- The daily energy efficiency of single slope passive solar still varies with change of water depth for the same total daily solar intensity. The maximum energy efficiency of 30.97% was obtained from 1-cm water depth. The daily energy efficiency decreases from 30.97 to 19.21% when the water depth increases from 1 to 2.5 cm.
- Compared with daily energy efficiency, the daily exergy efficiency value is very low. For the same total daily solar intensity the daily exergy efficiency varies from 3.48 to 1.81% for increasing

water depth from 1 to 2.5 cm. The lower exergy efficiency as compared with energy efficiency is due to the significant degradation of energy quality.

- The exergy destruction of the basin liner, saline water, and glass cover is 3343.86, 826.36, and 232.87 W/m<sup>2</sup>/d, respectively, corresponding to the total daily solar exergy input of 5813.35 W/m<sup>2</sup> for 1-cm water depth.
- It is observed that within the different components the largest exergy destruction takes place in the basin liner. The exergy destruction of basin liner to be decreased by selecting proper material for basin liner which leads to improve the exergy efficiency of solar still.

## Nomenclature

$m_w$	—	hourly distillate yield (kg)
$M_w$	—	daily distillate yield (kg)
$L$	—	latent heat of vaporization (J/kg)
$A_s$	—	basin area of solar still (m <sup>2</sup> )
$I_{t(s)}$	—	hourly incident solar radiation (W/m <sup>2</sup> )
$\sum I_{t(s)}$	—	total incident solar radiation (W/m <sup>2</sup> /d)
$\sum \dot{E}_{x_{in}}$	—	exergy input of solar still (W)
$\sum \dot{E}_{x_{out}}$	—	exergy output of solar still (W)
$\sum \dot{E}_{x_{dest}}$	—	exergy destructed in solar still (W)
$\sum \dot{E}_{x_{sun}}$	—	exergy input from the sun on solar still (W)
$\sum \dot{E}_{x_{evap}}$	—	exergy evaporated on solar still (W)
$\sum \dot{E}_{x_{work}}$	—	exergy work rate for solar still (W)
$\eta_{Ex}$	—	exergy efficiency (%)
$\eta_{energy}$	—	daily energy efficiency (%)

$\omega_{\text{energy}}$	— mathematical uncertainty of energy efficiency (%)
$\omega_{\text{exergy}}$	— mathematical uncertainty of exergy efficiency (%)
$T_a$	— ambient air temperature (K)
$T_w$	— water temperature (K)
$T_b$	— basin temperature (K)
$T_{gi}$	— inner glass temperature (K)
$T_{go}$	— outer glass temperature (K)
$T_{\text{sky}}$	— sky temperature (K)
$E_{x_{\text{des},b}}$	— exergy destruction from basin liner ( $\text{W}/\text{m}^2$ )
$E_{x_{\text{des},w}}$	— exergy destruction from saline water ( $\text{W}/\text{m}^2$ )
$E_{x_{\text{des},g}}$	— exergy destruction from glass cover ( $\text{W}/\text{m}^2$ )
$E_{x_{\text{ins}}}$	— exergy loss through insulation ( $\text{W}/\text{m}^2$ )
$E_{x_w}$	— exergy utilized to heat saline water ( $\text{W}/\text{m}^2$ )
$E_{x_{l,w-g}}$	— total exergy associated with saline water and glass cover ( $\text{W}/\text{m}^2$ )
$E_{x_{e,w-g}}$	— exergy associated with saline water and glass cover through evaporation ( $\text{W}/\text{m}^2$ )
$E_{x_{c,w-g}}$	— exergy associated with saline water and glass cover through convection ( $\text{W}/\text{m}^2$ )
$E_{x_{r,w-g}}$	— exergy associated with saline water and glass cover through radiation ( $\text{W}/\text{m}^2$ )
$E_{x_{l,g-a}}$	— total exergy associated with glass cover and atmosphere ( $\text{W}/\text{m}^2$ )
$E_{x_{c,g-a}}$	— exergy associated with glass cover and atmosphere through convection ( $\text{W}/\text{m}^2$ )
$E_{x_{r,g-a}}$	— exergy associated with glass cover and atmosphere through radiation ( $\text{W}/\text{m}^2$ )
$h_w$	— convective heat transfer between basin liner and water ( $\text{W}/\text{m}^2\text{K}$ )
$h_b$	— overall heat transfer between basin liner and atmosphere ( $\text{W}/\text{m}^2\text{K}$ )
$h_{e,w-g}$	— evaporative heat transfer coefficient between saline water and glass cover ( $\text{W}/\text{m}^2\text{K}$ )
$h_{c,w-g}$	— convective heat transfer coefficient between saline water and glass cover ( $\text{W}/\text{m}^2\text{K}$ )
$h_{r,w-g}$	— radiative heat transfer coefficient between saline water and glass cover ( $\text{W}/\text{m}^2\text{K}$ )
$h_{c,g-a}$	— convective heat transfer coefficient between glass cover and atmosphere ( $\text{W}/\text{m}^2\text{K}$ )
$h_{r,g-a}$	— radiative heat transfer coefficient between glass cover and atmosphere ( $\text{W}/\text{m}^2\text{K}$ )
$V$	— wind velocity in (m/s)

### Symbols

$\alpha_g$	— absorptivity of glass cover
$\alpha_b$	— absorptivity of basin liner
$\alpha_w$	— absorptivity of water
$\tau_g$	— transmissivity of glass cover
$\tau_w$	— transmissivity of water
$\epsilon_{\text{eff}}$	— effective emissivity
$\sigma$	— Stefan—Boltzmann constant
$\omega$	— uncertainty

### References

- [1] J. Joseph, R. Saravanan, S. Renganarayanan, Studies on a single-stage solar desalination system for domestic applications, *Desalination* 173 (2005) 77–82.
- [2] A. Kaushal, Varun, Solar stills: A review, *Renewable Sustainable Energy Rev.* 14 (2010) 446–453.
- [3] V. Sivakumar, E. Ganapathy Sundaram, Improvement techniques of solar still efficiency: A review, *Renewable Sustainable Energy Rev.* 28 (2013) 246–264.
- [4] J.C. Torchia-Nunez, M.A. Porta-Gandara, J.G. Cervantes-de Gortari, Exergy analysis of a passive solar still, *Renewable Energy* 33 (2008) 608–616.
- [5] G.N. Tiwari, V. Dimri, A. Chel, Parametric study of an active and passive solar distillation system: Energy and exergy analysis, *Desalination* 242 (2009) 1–18.
- [6] V.K. Dwivedi, G.N. Tiwari, Experimental validation of thermal model of a double slope active solar still under natural circulation mode, *Desalination* 250 (2010) 49–55.
- [7] S. Kumar, G.N. Tiwari, Analytical expression for instantaneous exergy efficiency of a shallow basin passive solar still, *Int. J. Therm. Sci.* 50 (2011) 2543–2549.
- [8] S. Shanmugan, V. Manikandan, K. Shanmugasundaram, B. Janarathanan, J. Chandrasekaran, Energy and exergy analysis of single slope single basin solar still, *Int. J. Ambient Energy* 33(3) (2012) 142–151.
- [9] A. Kianifar, S. Zeinali Heris, O. Mahian, Exergy and economic analysis of a pyramid-shaped solar water purification system: Active and passive cases, *Energy* 38 (2012) 31–36.
- [10] A.K. Sethi, V.K. Dwivedi, Exergy analysis of double slope active solar still under forced circulation mode, *Desalin. Water Treat.* 51 (2013) 7394–7400.
- [11] K.R. Ranjan, S.C. Kaushik, N.L. Panwar, Energy and exergy analysis of passive solar distillation systems, *Int. J. Low-Carbon Technol.* (2013) 1–11. Available from: <http://ijlct.oxfordjournals.org/content/early/2013/09/26/ijlct.ctt069.full.pdf+html>.
- [12] K.R. Ranjan, S.C. Kaushik, Energy, exergy and thermo-economic analysis of solar distillation systems: A review, *Renewable Sustainable Energy Rev.* 27 (2013) 709–723.
- [13] H. Aghaei Zoori, F. Farshchi Tabrizi, F. Sarhaddi, F. Heshmatnezhad, Comparison between energy and exergy efficiencies in a weir type cascade solar still, *Desalination* 325 (2013) 113–121.
- [14] O. Ansari, M. Asbik, A. Bah, A. Arbaoui, A. Khmou, Desalination of the brackish water using a passive solar still with a heat energy storage system, *Desalination* 324 (2013) 10–20.
- [15] F. Nematollahi, A. Rahimi, T. Tavakoli Gheinani, Experimental and theoretical energy and exergy analysis for a solar desalination system, *Desalination* 317 (2013) 23–31.
- [16] R. Saidur, G. BoroumandJazi, S. Mekhlif, M. Jameel, Exergy analysis of solar energy applications, *Renewable Sustainable Energy Rev.* 16 (2012) 350–356.
- [17] G. BoroumandJazi, R. Saidur, B. Rismanchi, S. Mekhilef, A review on the relation between the energy and exergy efficiency analysis and the technical characteristic of the renewable energy systems, *Renewable Sustainable Energy Rev.* 16 (2012) 3131–3135.

- [18] U. Lucia, Entropy and exergy in irreversible renewable energy systems, *Renewable Sustainable Energy Rev.* 20 (2013) 559–564.
- [19] S. Kumar, G.N. Tiwari, Thermal modelling, validation and exergetic analysis of a hybrid Photovoltaic/Thermal (PV/T) active solar still, *Int. J. Exergy* 6(4) (2009) 567–591.
- [20] A. Hepbalsi, A key review on exergetic analysis and assessment of renewable energy sources for a sustainable future, *Renewable Sustainable Energy Rev.* 12(3) (2008) 593–661.
- [21] I. Dincer, M.A. Rosen, *Exergy: Energy, Environment and Sustainable Development*, 1st ed., Elsevier Ltd., London, 2007, pp. 36–59.
- [22] Y.H. Zurigat, M.K. Abu-Arabi, Modelling and performance analysis of a regenerative solar desalination unit, *Appl. Therm. Eng.* 24 (2004) 1061–1072.
- [23] R.V. Dunkle, Solar Water Distillation, The Roof Type Solar Still and a Multi Effect Diffusion Still, *Internal Developments in Heat Transfer, A.S.M.E.*, in: *Proceedings of International Heat Transfer, Part V*, University of Colorado, Boulder, CO, 1961, pp. 895–902.
- [24] J.L. Fernandez, N. Chargoy, Multi stage indirectly heated solar still, *Solar Energy* 44(4) (1990) 215–223.
- [25] S.K. Shukla, V.P.S. Sorayan, Thermal modeling of solar stills: An experimental validation, *Renewable Energy* 30 (2005) 683–699.
- [26] E. Sartori, Solar still versus solar evaporator: A comparative study between their thermal behaviors, *Solar Energy* 56(2) (1996) 199–206.
- [27] W.H. McAdams, *Heat Transmission*, 3rd ed., McGraw-Hill Book Company, New York, NY, 1954.
- [28] W.C. Swinbank, Long-wave radiation from clear skies, *Quarterly J. Royal Meteorol. Soc.* 89 (1963) 339–348.
- [29] J.P. Holman, *Experimental Methods for Engineers*, 8th ed., McGraw Hill Publications, New York, NY, 2012, pp. 62–65.
- [30] V.K. Dwivedi, G.N. Tiwari, Annual energy and exergy analysis of single and double slope passive solar stills, *Trends Appl. Sci. Res.* 3(3) (2008) 225–241.